

DIODE LESS T-NPC INVERTERS FED DIRECT TORQUE CONTROL DOUBLE-STATOR-WINDING PMSM DRIVE WITH VECTOR SPACE DECOMPOSITION

¹B Santhosh Kumar, ²M Praveen Kumar, ³Neerati Rajashekar

¹Assistant professor, Department of Electrical and Electronics Engineering, Trinity College Of Engineering And Technology

Abstract-This paper presents the three level diode less T-shaped neutral point clamped multilevel inverter with vector space decomposition (VSD) based direct torque control (DTC) scheme fed double stator-winding PMSM drive, which delivers an active solution for high-power high consistency applications. Good dynamic response and harmonic performance are obtained by suggesting a modest but effective space vector modulation (SVM) for DTC of T-NPC double-stator-winding drives based two-step voltage vector synthesis. To conquer the conceivable harmonics persuaded from instable parameters in phase windings and from the induced back emf in electrical machines by integrating the closed loop controllers on harmonic subspace. Furthermore, for fault tolerant operation of the diode less T-NPC multilevel double-stator-winding PMSM drives by using hybrid current control with one-phase is open. In the hybrid current controller, the healthy winding still uses the SVM-DTC control while the faulty winding uses the closed-loop current controller to track the optimized current references. The simulation results are carried out on a MATLAB/SIMULATION software to authenticate the strength and performance of the proposed fault tolerant control schemes.

Keywords: vector space decomposition, direct torque control, space vector modulation, diode less-T shaped multilevel inverter

I. Introduction

WITH the increasing demands of higher precision machine drives, AC machine drives, which are widely considered as a substitute of direct current (DC) machine drives, are deemed as the most prevailing components of modern motion control systems due to many distinctive features they offer. Among various AC machine drives, PMSM has been receiving abundant attention because of its advantageous features including high efficiency, high power density, large torque-to-inertia ratio, low noise, and free maintenance [1]– [4]. As such, PMSM drives have been extensively applied to a variety of industrial sectors, such as robotics, machine tools, electrical vehicles, power generations and aerospace [3].

Despite many advantages described above, high precision control of PMSM drives is rather challenging because the motion dynamics of PMSM are complicated and intrinsically nonlinear, and, in addition, subject to various sources of disturbances and uncertainties [5]–[7]. Aiming to achieve desired servo control performance, apart from classical proportional-integral-derivative (PID) controllers, plenty of advanced control algorithms have been put forward for AC machine drives, for example, model predictive control [4], [8], [9], robust and adaptive control [10] internal model control output regulation [2], disturbance observer-based control (DOBC) [3],[4], and active disturbance rejection control (ADRC) [9], to name but a few. When the phase number is multiples of three, the standard “off-the-shelf” power converters can be used.

So, the drives with multiple stator windings are regarded preferable for multiphase systems [6].

In order to increase the reliability of the drives, the multiple stator windings could be designed with no magnetic coupling. In such a way, faults in one conversion channel have little impact on operation of other conversion channels. To achieve this goal, multiple three-phase windings can be distributed in well-defined parts of one stator [7]. In particular, the stator permanent-magnet (PM) machines are proposed to achieve magnetic decoupling among different groups of windings by allocating PM magnets and redundant teeth in stators [8].

Secondly, the multiple stator windings can also be mounted in multiple stators sharing a common rotor to achieve magnetic decoupling. This multi-stator machine configuration enable the physical separation among multiple stator windings [9]. Thirdly, the multiple stator windings can be located in separate motors, whose rotors are coupled mechanically. This multi-motor drive can be applied, where the high-power motor is difficult to realize for strong attractive force of magnet material and heating problem [10]. Normally, the multiple stator windings of the drive are controlled separately, and they are required to track these separate current references to share the total torque of the drive

Recently, intensive research on vector space decomposition (VSD) method have been developed for multiphase drives, where the fundamental components, harmonic components and zero-sequence components are decomposed into orthogonal subspaces respectively. An

obvious merit of this method is that the electro-mechanical torque of the drive can be regulated as a whole by controlling components on fundamental subspace, while the harmonic components are limited by optimizing the switching vectors on harmonic component subspace. For further suppressing the low-order harmonics and the unbalanced currents between the multiple windings, additional harmonic current controllers are required on the harmonic current subspace. The model predictive control and the decoupling control are proposed based on VSD to achieve fast dynamic performance for multiphase drives. The direct torque control (DTC), both the table-based DTC (ST-DTC) and the SVM based DTC schemes have also been proposed for the drives with dual three-phase windings. To suppress the current harmonics, an additional switching table and a flux estimator on x-y plane are added, and a two-step ST-DTC scheme is proposed for the dual three-phase PMSM drives. To avoid increasing complexity of the DTC strategy, new 12 switching vectors are synthesized by voltage vectors from two dodecagons with different amplitudes. To the best of authors' knowledge, all these VSD based control are with two-level inverters fed multiphase drives.

The T-NPC three-level inverters become more popular for low-voltage and high-reliability applications due to their superior harmonic performance and better fault tolerant control capability [9-10]. Table I compares the performance of T-NPC three-level topology with two-level topology and diode clamped NPC (D-NPC) three-level topology. The T-NPC three-level inverter offers the advantages of low voltage harmonics, small common-mode voltage, small electromagnetic interference (EMI), high efficiency and high fault tolerant capability. Since the power switch in half bridge withstand full voltage of DC link, the T-NPC three-level inverter is suitable for low-voltage applications compared to D-NPC three-level inverter. In terms of open-switch faults, the faulty leg in two-level inverter has to be removed completely. For D-NPC three-level inverter, the faulty leg is also useless when one inner switch of the leg is open. Compared to them, the faulty leg of T-NPC three-level inverter can still be used for fault tolerant control, no matter which switch breaks down. In case of an open-phase fault, the faulty phase can be connected to neutral point of DC link in three-level inverter through circuit reconstruction. The three-level inverter has good control over neutral point voltage, which is difficult for two-level inverter to balance.

Table .1

Performance Comparison

S.No	Compare Name	Two-Level	D-NPC Three Level Inverter	T-NPC Three Level Inverter
1	IGBT Voltage	V_{dc}	$V_{dc}/2$	$V_{dc}/2, V_{dc}$
2	Harmonics	High	Low	Low
3	Loss (5-30 kHz)	Large	Middle	Small
4	EMI	Large	Small	Small
5	Fault Tolerant Capability	Low	Middle	High

1	IGBT Voltage	V_{dc}	$V_{dc}/2$	$V_{dc}/2, V_{dc}$
2	Harmonics	High	Low	Low
3	Loss (5-30 kHz)	Large	Middle	Small
4	EMI	Large	Small	Small
5	Fault Tolerant Capability	Low	Middle	High

II. Configuration And Modelling

Fig. 1 shows the configuration of the T-NPC double-stator-winding PMSM drive, where a six-phase T-NPC inverter feeds a PMSM drive system with two stator windings. Similar to two-level voltage source inverters, the T-NPC inverters have one switch S1 in the upper leg, and another one S4 in the lower leg for each phase. Besides, there are two neutral-point-clamping switches S2 and S3, which block half of the DC link voltage. Since the output phase could be clamped to the mid-point of DC link through switches S2 and S3, the inverter can output three voltage levels of $+U_{dc}/2, 0$ and $-U_{dc}/2$. The electrical angle between the double three-phase windings could be in-phase, with 30° shifted angle or 60° shifted angle.

In this paper, the shifted angle is chosen as 30° , and two neutrals of windings are isolated for eliminating the zero-sequence currents inherently.

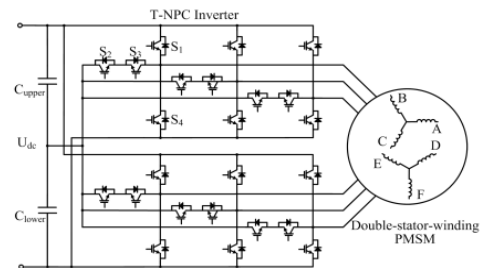


Fig. 1. Configuration of T-NPC double-stator winding PMSM drive

III. Proposed DTC Based On VSD

Fig. 2 shows the proposed DTC scheme for the T-NPC double-stator-winding PMSM drive based on a two-step voltage vector synthesis SVM. By using the two-step SVM, the design and implementation of switching and control strategies become more convenient. With the feedback of voltage and current components in α - β subspace, the electromagnetic torque T_e and the stator flux ψ_s are estimated.

Based on the stator flux error between the reference value and the estimated one, the voltage reference for DTC control are obtained. With the amplitude V_{ref} and position θ of voltage reference, the switching signals are generated by the two-step SVM at the first stage. Then, the final switching signals are obtained by incorporating the voltage

perturbation from the closed-loop current controllers on x-y subspace. The components on x-y subspace might be induced by back EMF and asymmetry of machine winding, which will cause additional loss and unbalance in phase currents. So, the closed-loop control is used to regulate x-y current components to suppress them to be zero. The encoder is used to measure the rotor speed, and the closed-loop speed controller generates the torque reference T_{e_ref} .

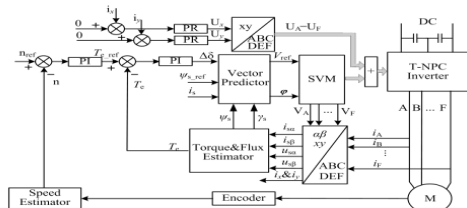


Fig.2. Control diagram of the proposed VSD based DTC for T-NPC three-level inverters fed double-stator-winding PMSM

IV. Fault Tolerant Control

A. Proposed Fault Tolerant Control Structure

As aforementioned, the double-stator-winding PMSM drives can offer high fault tolerant capability due to the redundant phase legs. Both the short circuit and the open-circuit faults can become open-circuit conditions by using fuses or circuit breakers. When the fault occurs, the degraded operation could work by removing the faulty winding completely, and the other healthy winding continues working. Actually, if only one phase is forced open in the faulty winding, the remaining two phases can still produce torque. In this paper, a hybrid fault tolerant control is proposed for the double-stator-winding PMSM drive under one-phase open conditions. The aim is to make full use of remaining phase legs to achieve good operating performance such as fast dynamic performance, small torque ripple and low copper loss under faulty conditions. Fig. 3 shows the block diagram of the proposed hybrid fault tolerant control scheme for open-circuit fault in phase D. The healthy three-phase winding (A, B and C) still uses the SVM-DTC to achieve closed-loop control of torque while the phases of faulty winding (E and F) adopt closed-loop current controller to track the optimized current references for minimum copper loss under fault tolerant operation.

Therefore, the calculation of stator flux is modified based on current model as shown in Fig. 4. The current model is convenient to calculate the stator flux even with open-circuit faults in phase windings. The closed-loop speed controller generates the total torque reference T_{e_ref} for the double-stator-winding PMSM machine, and the value will be used for controlling both the healthy three-phase winding (A, B and C) and the faulty three-phase winding (E and F). By using closed-loop control of torque in drive system with healthy three-phase winding (A, B and C), the

torque pulsation caused by faulty winding (E and F) can be compensated well in the electrical machine.

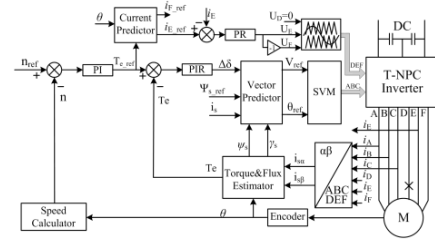


Fig. 3. Block diagram of hybrid fault tolerant control for T-NPC double-stator-winding PMSM drive.

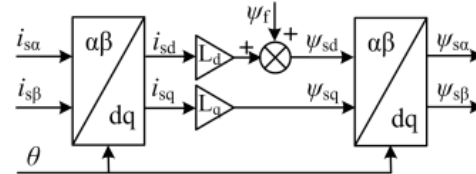


Fig. 4. Calculation of stator flux based on current model.

The three-phase SVM scheme for three-level inverter is used for the three-phase healthy winding. The balance of the upper and the lower capacitor voltages in DC link is achieved by adjusting dwelling time of redundant small vectors of healthy three-phase winding. It is noted that the angle deviation $\Delta\delta$ consists of both DC component and periodic components since the healthy winding has to compensate the double-frequency torque pulsation in the faulty winding. So, a resonant control is used together with the PI controller for the torque controller.

V. Simulation Results

Simulation Verification

At first, the MATLAB/Simulink is used to simulate the performance of the T-NPC three-level double-stator-winding PMSM drive. In the simulation, there is magnetic coupling between double stator windings and there is a 30-degree shifted angle between them. The key parameters of the drive system in simulation are given in Table V. Fig. 5(a)-(c) show the simulated steady-state waveforms under 1400 rpm and 20 Nm. In Fig. 5(a)-(c), five-level phase-to-phase inverter output voltages, steady stator flux trajectory and six-phase currents waveforms are observed. Due to the proposed harmonic-free SVM, the harmonics of stator currents are low. Fig. 5(d)-(h) show the transient performance of drive while the rotor speed is changed between 500 rpm and 1000 rpm. It verifies that the actual torque and speed can track their reference values accurately and quickly. The torque ripple is smaller than 0.3 Nm throughout the process. During the transient process, the harmonic components of currents on x-y subspace are limited low and the maximum amplitude is below 0.4 A, in Fig. 5(g). The upper and lower capacitor voltages in DC link are controlled well and the difference

in their values is less than 2V in Fig.5(h) by using the proposed switching strategy.

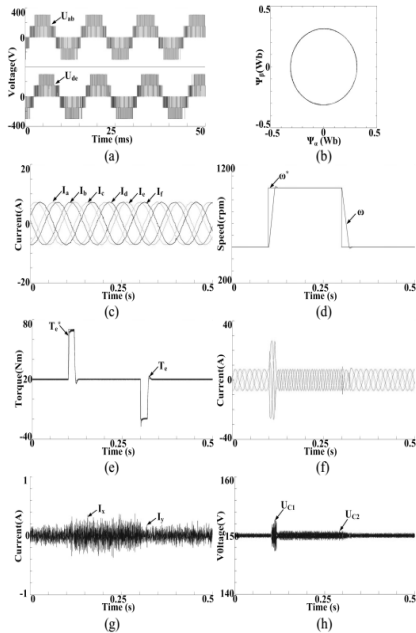


Fig. 5. Simulated performance of drive under normal condition: (a) inverter output voltage waveform; (b) stator flux trajectory; (c) stator currents; (d) rotor speed; (e) torque; (f) stator currents; (g) harmonics on x-y subspace; (h) DC link capacitor voltages.

Fig. 6 shows the effects of the closed-loop controllers on x-y subspace for suppressing harmonics from back EMF and asymmetry of machine winding. By adding the 5th order harmonics in back EMF, the obvious current ripples appear in components on x-y subspace without the closed-loop controller while the current harmonics are suppressed effectively by incorporating the closed-loop controller in Fig. 6(a). Accordingly, the fifth order harmonics in stator currents induced from back EMF are controlled well in Fig. 6(b). Fig. 6(c) and (d) show that the asymmetrical currents can be controlled balanced with the closed-loop controllers on x-y subspace after purposely increasing 1Ω resistor in phase A.

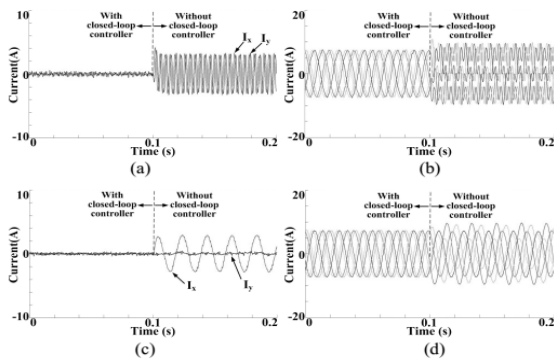


Fig. 6. Simulated performance of closed-loop current controller on x-y subspace: (a) x-y current components with 5th harmonics in back EMF; (b) stator currents with 5th harmonics in back EMF; (c) x-y current components with asymmetric resistor in phase A; (d) stator currents with asymmetric resistor in phase A.

Fig. 7 shows the drive performance using SVM-DTC without fault tolerant control when phase D is in open-circuit fault. The obvious torque ripple is observed after the fault is introduced in Fig. 7(a) since optimization of torque ripple is not considered in standard SVM-DTC of normal condition.

Fig. 7(c) and (d) show the dynamic performance of the drive under D-phase open-circuit fault without fault tolerant control scheme. The obvious torque ripple is observed although the upper capacitor voltage and the lower capacitor voltage in DC link are controlled balanced. On the other hand, Fig. 8 shows the drive performance with the proposed fault tolerant control in last section. As shown in Fig. 8(a), the steady-state torque is smooth because the SVM-DTC of healthy winding can compensate the torque oscillation induced from the faulty winding well. The corresponding steady-state current waveforms are shown in Fig. 8(b). Fig. 8(c) and (d) show the dynamic performance of the drive with fault tolerant control under D-phase open-circuit fault. The upper capacitor voltage and the lower capacitor voltage in DC link are controlled well with redundant vectors.

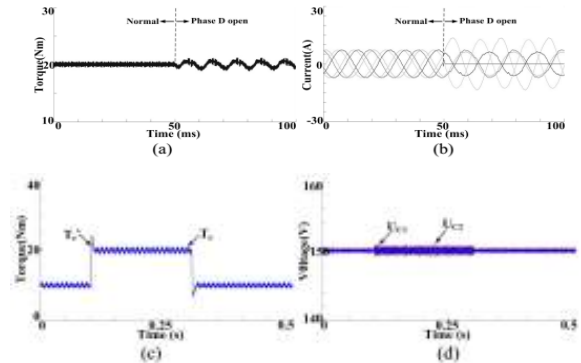


Fig. 7. Simulated performance of drive with standard SVM-DTC under one-phase open-circuit fault: (a) torque; (b) stator currents; (c) torque during transient process; (d) DC link capacitor voltages during transient process.

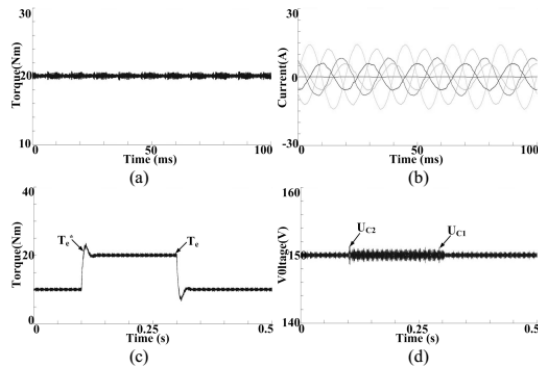


Fig. 8. Simulated performance of drive with proposed fault tolerant control under one-phase open-circuit fault: (a) torque; (b) stator currents; (c) torque during transient process; (d) DC link capacitor voltages during transient process.

VI. Conclusions

In this paper, the VSD based DTC control schemes are studied and proposed for T-NPC three-level inverters fed double-stator-winding PMSM drives. To simplify the algorithm and maintain good harmonic performance, a two-step voltage vector synthesis SVM strategy is proposed for the six-phase T-NPC inverters, which is in turn applied for the SVM-DTC scheme. Three groups of harmonic-free voltage vectors are composed from five original voltage vector groups by forcing their average volt-seconds on x-y subspace to be zero. Then, the new three groups of harmonic-free voltage vectors are used in synthesis of final voltage reference. In addition to the merits of easy implementation and elimination of low order harmonics, the proposed two-step voltage vector synthesis based SVM can suppress the mid-point voltage fluctuation in DC link by using redundant voltage vectors. An additional current controller on x-y subspace has been designed to generate the perturbation for the switching pulses, which functions to further suppress the harmonics from back EMF and asymmetry of machine winding. To fully utilize high fault tolerant capability of double-stator-winding drives under one-phase open-circuit fault, a hybrid current controller has been proposed in this paper, where the healthy winding still uses the SVM-DTC control while the faulty winding uses the closed-loop current controller to track the optimized current references. Not only the torque ripple can be suppressed under fault conditions, but also the minimum copper loss can be achieved with the optimized current references. The fluctuation of mid-point voltage in DC link is controlled well with redundant voltage vectors of the healthy three-phase winding. The computer simulation is used to verify the control performance of the double-stator-winding PMSM drive with magnetic coupling, and the experiments are applied to verify the control performance of the PMSM drive with two magnetically isolated three-phase windings. Both of them have verified that the proposed switching

strategies and control schemes could offer good operating performance under normal and faulty conditions

References

- [1] S. Li and Z. Liu, "Adaptive speed control for permanent-magnet synchronous motor system with variations of load inertia," *IEEE Trans. Ind. Electron.*, vol. 56, no. 8, pp. 3050–3059, Aug. 2009.
- [2] Y. A.-R. I. Mohamed and E. El-Saadany, "A current control scheme with an adaptive internal model for torque ripple minimization and robust current regulation in pmsm drive systems," *IEEE Trans. Energy Convers.*, vol. 23, no. 1, pp. 92–100, Mar. 2008.
- [3] Y. A.-R. I. Mohamed, "Design and implementation of a robust current control scheme for a pmsm vector drive with a simple adaptive disturbance observer," *IEEE Trans. Ind. Electron.*, vol. 54, no. 4, pp. 1981–1988, Aug. 2007.
- [4] R. Errouissi, M. Ouhrouche, W.-H. Chen, and A. Trzynadlowski, "Robust cascaded nonlinear predictive control of a permanent magnet synchronous motor with antiwindup compensator," *IEEE Trans. Ind. Electron.*, vol. 59, no. 8, pp. 3078–3088, Aug. 2012.
- [5] Z. Zhu, S. Ruangsinchaiwanich, and D. Howe, "Synthesis of cogging torque waveform from analysis of a single stator slot," *IEEE Trans. Ind. Appl.*, vol. 42, no. 3, pp. 650–657, May. 2006.
- [6] W. Qian, S. Panda, and J.-X. Xu, "Torque ripple minimization in pm synchronous motors using iterative learning control," *IEEE Trans. Power Electron.*, vol. 19, no. 2, pp. 272–279, Mar. 2004.
- [7] S.-H. Hwang and J.-M. Kim, "Dead time compensation method for voltage-fed pwm inverter," *IEEE Trans. Energy Convers.*, vol. 25, no. 1, pp. 1–10, Mar. 2010.
- [8] R. Errouissi, M. Ouhrouche, W.-H. Chen, and A. Trzynadlowski, "Robust nonlinear predictive controller for permanent-magnet synchronous motors with an optimized cost function," *IEEE Trans. Ind. Electron.*, vol. 59, no. 7, pp. 2849–2858, Jul. 2012.
- [9] H. Liu and S. Li, "Speed control for pmsm servo system using predictive functional control and extended state observer," *IEEE Trans. Ind. Electron.*, vol. 59, no. 2, pp. 1171–1183, Feb. 2012.
- [10] F. El-Sousy, "Hybrid H1-based wavelet-neural-network tracking control for permanent-magnet synchronous motor servo drives," *IEEE Trans. Ind. Electron.*, vol. 57, no. 9, pp. 3157–3166, Sep. 2010.